Available online at www.sciencedirect.com
SCIENCE DIRECT
Journal of Nuclear Materials 355 (2006) 30–37
journal of nuclear materials
www.elsevier.com/locate/jnucmat

Dynamic strain ageing in prior cold worked 15Cr–15Ni titanium modified stainless steel (Alloy D9)

K.G. Samuel *, S.K. Ray, G. Sasikala

Materials Technology Division, Indira Gandhi Centre for Atomic Research, Kalpakkam 603 102, India

Received 17 December 2005; accepted 27 March 2006

Abstract

Dynamic strain ageing (DSA) behavior of a 20% prior cold worked titanium modified austenitic stainless steel (Alloy D9) was investigated in the temperature range 300–1023 K at a constant (nominal) strain rate of $1.33 \times 10^{-3}\ s^{-1}$. Serrated plastic flow was observed in a narrow temperature region of 773–873 K. Anomalies characteristic of DSA were observed in the variations of strength, ductility, and strain hardening parameters with temperature. Specifically, the difference between ultimate tensile stress and yield stress indicated that a single DSA mechanism is operative over the range of observations. Plastic strain energy density for uniform deformation showed a peak in the DSA temperature range, suggesting that in this material, DSA should enhance the ductile fracture resistance.

1. Introduction

The material for the present investigation, a fully austenitic 15Cr–15Ni titanium modified stainless steel (Alloy D9), has been developed for applications as fuel pin and wrapper material for sodium cooled fast nuclear reactors, by adjusting the composition of Type 316 stainless steel, from the considerations of good combination of high temperature tensile and creep strength properties, irradiation creep resistance and resistance to irradiation induced void swelling [1–5]. This alloy contains controlled additions of silicon, titanium, higher levels of nickel and lower level of chromium. Minor elements having large neutron absorption cross-section, and impurities affecting weldability are kept to a minimum. Induction vacuum melting followed by vacuum arc refining is specified to achieve the required cleanliness. In order to improve the swelling resistance, efficient traps for vacancies and helium such as dislocations and precipitate–matrix interfaces have been introduced by adjusting alloy chemistry and by way of prior cold work.

The typical operating temperature of the hexagonal wrapper tube of the fuel subassembly is in the range 673–873 K. This operating temperature range falls in the regime of dynamic strain ageing (DSA) for austenitic stainless steels, arising from dynamic interaction between solute atoms and dislocations. Specifically, in tensile deformation, it may manifest as serrated or jerky flow. It begins after a finite amount of critical strain in many solid solution

* Corresponding author.
E-mail address: samuel@igcar.ernet.in (K.G. Samuel).

0022-3115/$ - see front matter © 2006 Elsevier B.V. All rights reserved.
doi:10.1016/j.jnucmat.2006.03.016

alloys. The temperature regime of serrated flow has been found to depend on the chemistry [6,7], strain rate [6,8], and grain size [9]. Other manifestations of DSA in tensile deformation are [10]: in the temperature regime for DSA, plots against test temperature for flow stress, work hardening rate, work hardening coefficient and Hall–Petch constant show anomalous peaks, and those for ductility and strain rate sensitivity show dips. Rodriguez [10] systematically catalogued these various manifestations including the types of serrations observed, and also described the various physical processes involved in DSA and serrated plastic flow. Though DSA has been investigated in alloy D9 in the solution annealed condition with different Ti/C ratio over a wide range of temperature and strain rate [11], investigation on a prior cold worked condition has not been reported so far. The present paper aims at exploring the influence of prior cold work on DSA in alloy D9, as manifested in constant (nominal) strain rate tensile tests.

2. Experimental

Chemical composition (wt%) of the material investigated was C: 0.045, Cr: 13.88, Ni: 15.24, Mo: 2.12, Ti: 0.23, B: 12 ppm, Mn: 2.12, Si: 0.64, Cu: 0.017, As: 0.0019, N: 0.0021, Al: 0.01, Co: 0.007, S: <0.005, P: <0.005, Nb: <0.005, V: <0.01, Ta: <0.01. The dimensions of the hexagonal wrapper tube were 131.3 mm across flat faces and 3.2 mm thickness. The tubes have been procured in $20 \pm 4\%$ cold worked condition. Tensile specimen blanks were cut from the flat faces of the wrapper tube with tensile axis parallel to the length of the tube. Flat tensile specimens having 25 mm gauge length and 4.5 mm gauge width as shown in Fig. 1 were machined from the blanks.

Isothermal tensile tests were carried out in an Instron 1195 universal testing machine in the temperature range 300–1023 K at constant cross head speed of 2 mm per minute (nominal strain rate = $1.33 \times 10^{-3}\ s^{-1}$). Elevated temperatures for testing were achieved by employing a three zone resistance-heating furnace and the test temperature was controlled within ±2 K on the gauge length. The load and elongation were recorded using chart drive attached with the machine. The property data reported in this paper are average from at least two tests.

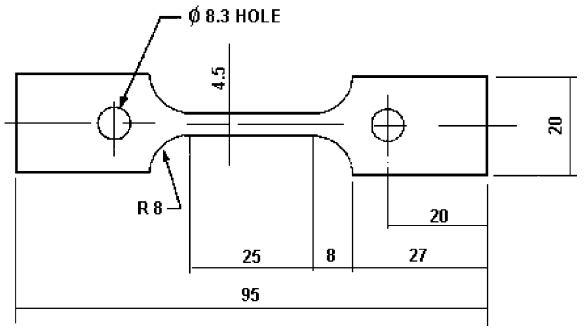

Fig. 1. Tensile test specimen.

3. Results and discussion

3.1. Serrated flow

Typical segments of the load elongation curves depicting serrated flow in prior cold worked alloy D9 is shown in Fig. 2. Serrated yielding in the prior cold worked material was observed only in the temperature range 773–873 K. According to the classifications of type of serrations [10], type A/E serration [10] was observed at 773 K, while type A/C serration was observed at 823 and 873 K. At 823 and 873 K serration persisted beyond necking till fracture. This range may be compared with the range 573–873 K reported for both type SS 316 [9], and alloy D9 [11], (tested at a strain rate one order less than the strain rate employed in the present study), in solution annealed conditions. Now, with increasing strain rate, the temperature regime for serrated yielding shifts towards higher temperatures and also narrows down [8]. Therefore, the higher and narrower temperature regime for serrated flow in the present study compared to that reported for the solution annealed D9 [11] could arise from the combined effect of prior cold work and higher strain rate. Specifically, it could arise from the combined effect of lower number of solute atoms in solution (because of secondary precipitation at the test temperature) and decreased density of solutes at dislocation line due to increased dislocation density.

The critical strain ε_c associated with the onset of serrated yielding was evaluated from load elongation charts as the minimum true plastic strain ε for an appreciable load drop, arbitrarily fixed as 10 N. The variation of $\ln \varepsilon_c$ with $1/T$ is shown in Fig. 3. According to Cottrell's theory [12], this critical strain is necessary to enhance the diffusion coefficient of the solute species responsible for DSA to acquire a velocity large enough to diffuse to the mobile dislocations and form solute atmospheres, to impede the motion of dislocations. This event is accomplished with the aid of vacancies generated through

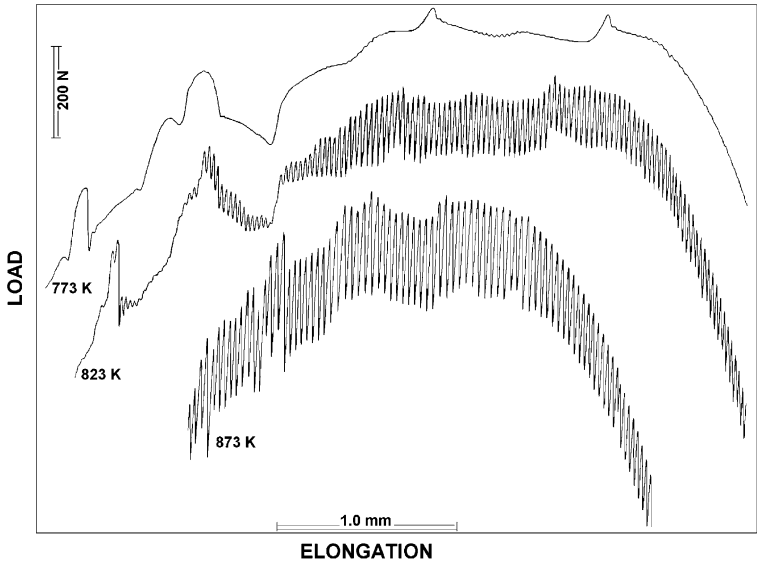

Fig. 2. Typical serrated flow in a prior cold worked alloy D9.

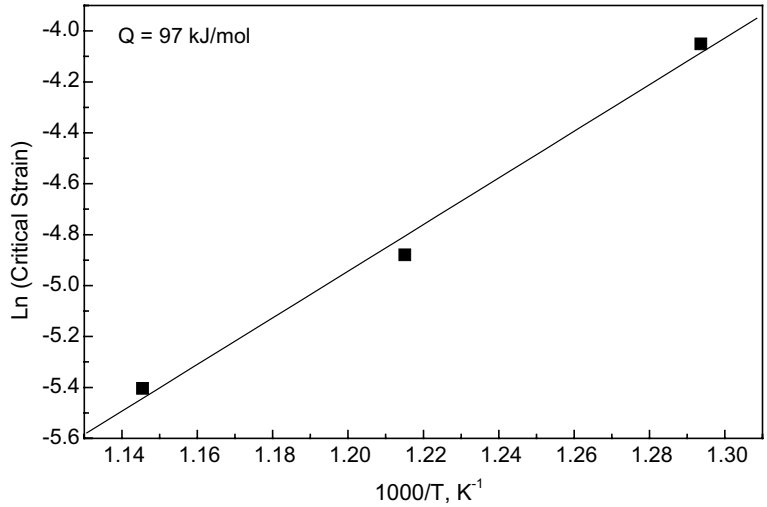

Fig. 3. Plot of ln (critical strain) vs reciprocal temperature used for Q determination.

plastic deformation. According to the formulation of McCormick [13], widely employed to determine the activation energy Q for solute diffusion based on the knowledge of the dependence of ε_c on (absolute) temperature T and strain rate $\dot{\varepsilon}$ in several alloys including austenitic stainless steels [14–19]:

$$\varepsilon_c^{m+\beta} = K' \cdot \dot{\varepsilon} \cdot \exp(Q/RT) \quad (1)$$

where m and β are the respective exponents in the relations for the variation of vacancy concentration C_v and mobile dislocation density ρ_m with plastic strain ($C_v \propto \varepsilon^m$, $\rho_m \propto \varepsilon^\beta$), K' is a constant, and R is the gas constant. Fig. 3 is thus consistent with Eq. (1), and can be used to determine Q if $(m+\beta)$ is known beforehand. $(m+\beta)$ can be obtained as the slope in the plot of $\ln\varepsilon_c$ against $\ln\dot{\varepsilon}$ at constant T; since in the present campaign, data were generated for a single $\dot{\varepsilon}$ level, $(m+\beta)$ could not be determined from the experimental data. Generally for DSA involving substitutional solutes, the value of $(m+\beta)$ between 2 and 3 has been obtained whereas for DSA due to interstitial solutes, $(m+\beta)$ is usually close to 1 [10]. In an 18-8 stainless steel $(m+\beta)$ was reported [20] to be 1.15 at 873 K. In

solution annealed alloy D9, $(m+\beta)$ was reported as 1.28 in the temperature range 723–873 K [14]. If the same value for $(m+\beta)$ is assumed for the present cold worked grade, then from the slope of Fig. 3, Q computes as 97 kJ mol^{-1}. Saada [21] suggested that $C_v \propto \varepsilon^{(n+1)}$ where n is the strain hardening exponent in the Hollomon work hardening relation [22]

$$\sigma = k\varepsilon^n \tag{2}$$

Here k is a material constant that varies with $\dot{\varepsilon}$ and T, as does n. Following this suggestion, Jovanovic et al. [23] evaluated m as $n+1$. In strain hardening materials n and β are always positive. It may be argued that the limiting values for β are 0 to 1. $\beta = 0$ corresponds to mobile dislocation density constant with plastic strain. $\beta = 1$ correspond to the mobile dislocation density increasing linearly with strain. If a proportionality between ε and ρ_m is assumed, then $\beta = n$. The values of n determined from the present test data (see below) thus could be used to estimate $m+\beta \approx 2n+1$, whence Q values for the three temperatures showing serrated flow could be estimated as shown in Table 1. It may be noted that negative values of β and $(m+\beta)$ have been reported in the literature [24,25]. This behavior is referred to as inverse Portevin–Le Chatelier (PL) effect, where ε_c decreases with increasing $1/T$; obviously present data do not correspond to inverse PL effect (Fig. 3). On the other hand, Kubin and Estrin [26] suggest that the interpretation based on negative β (i.e., decrease of ρ_m with ε) in the inverse P–L regime seems to be unlikely.

Comparing these estimated with the Q values for austenitic alloys reported in literature, Table 2, apparently interstitial solute diffusion would be identified as the mechanism responsible for DSA. The problem with this interpretation is: deformation produced vacancies should have no role for mechanisms involving interstitial diffusion through matrix or along dislocation cores, unless the mechanism is more complex and involves mobility of

Table 1
Activation energy values calculated at various test temperatures using $(m+\beta)$ derived from work hardening relation

Temperature, K	n	$m = n+1$	$\beta = 1$	$(m+\beta) = 2n+1$	Q, kJ/mol
773	0.1043	1.1043	0.1043	1.2086	91.9
823	0.1048	1.1048	0.1048	1.2096	90.0
873	0.0626	1.0626	0.0626	1.1252	85.6
773–873				1.28[a]	97

[a] Value as reported for solution annealed Alloy D9.

Table 2
Activation energy data for serrated yielding in austenitic alloys from published literature

Q, kJ/mol	Temperature (K)	Mechanism suggested	Material	Authors	Year	Ref.
210–340		Suzuki locking (Cr or Ni diffusion)	Cr–Ni–Mn alloy	Tamhankar et al.	1958	[38]
356–398	573–923	Cr + C interaction (Cr diffusion)	AISI 316	Barnby	1965	[39]
85	473	C–C or C-vacancy pair (vacancy diffusion)	High Ni alloy	Rose and Glover	1966	[40]
142	473–773	C-vacancy pair (vacancy migration + Cr binding energy)	AISI 330	Jenkins and Smith	1968	[19]
377	>773	Cr–C interaction (Cr diffusion)	AISI 330	Jenkins and Smith	1968	[19]
255	523–973	Solute interaction (Cr diffusion)	AISI 316	Mannan et al.	1983	[9]
132–136	473–673	Vacancy-interstitial pair (interstitial diffusion)	AISI 304	De Almeida et al.	1985	[41]
170	673–873	–	AISI 316	Blanc and Strudel	1985	[42]
191–198	673–1023	C–C pair interaction with Cr	AISI 304	De Almeida et al.	1985	[41]
133	523–623	Solute interaction (interstitial diffusion)	AISI 316	Samuel et al.	1988	[8]
278	673–923	Solute interaction (Cr diffusion)	AISI 316	Samuel et al.	1988	[8]
133–147	723–873	Schoeck–Seegar locking by C (or N) vacancy pair	Alloy D9	Venkadesan et al.	1992	[14]
106–124	573–623	Vacancy migration	Alloy D9	Venkadesan et al.	1992	[14]
171–185	773–923	Interaction of Ti with C and/or N	Alloy D9	Venkadesan et al.	1992	[14]
188	<873	N diffusion	High N Steel	Ilola et al.	1999	[43]
138.5	523–673	Interaction between (C, Ni) solute atom atmosphere and dislocation	18-8 stainless steel	Kaiping et al.	2004	[20]
173	723–853	Interaction between (C,Cr) solute atom atmosphere and dislocation	18-8 stainless steel	Kaiping et al.	2004	[20]
220	598–698	Cr diffusion	Duplex SS	Gironès et al.	2004	[44]
75–205	523–923	Pipe diffusion of solute atoms such as C, N, Cr	AISI316L	Seong-Gu Hong and Soon-Bok Lee	2005	[45]
97	773–873		Alloy D9 prior cold worked	Present work	2005	

interstitial–vacancy pairs, e.g. Schoeck–Seegar locking of dislocations by C (or N) vacancy pair as proposed by Venkadesan et al. [14] in this temperature range. It may therefore be concluded that the question of the activation energy for DSA in cold worked D9 is still open, and requires further study. We may however note here that as Table 2 indicates, the identification of the species that are responsible for DSA in the austenitic stainless steels of type AISI 316 or its variants is still a matter of controversy due to contradictory values found for the apparent activation energy for serrated yielding reported in the literature. It is however interesting to note that present estimates are lower than estimates of Q for DSA in solution annealed Alloy D9 reported in Table 2. The activation energy calculated is about 0.67–0.73 times the activation energy for lattice diffusion of C or N. Since solutes can diffuse rapidly along the dislocation core with an activation energy that may be 0.4–0.7 times the activation energy for lattice diffusion [27,28], it is possible that pipe diffusion of solute atoms (C, N) through the dislocation core is responsible for serrated yielding in this temperature range.

3.2. Strength and ductility properties

DSA manifests as anomalous variations, in the form of peaks or dips, of strength and ductility properties with temperature [6,8–11,28–30]. The temperature dependence of yield strength and ultimate tensile strength of the as received 20% cold worked material is shown in Fig. 4(a). Variations of yield strength and tensile strength with test temperature show similar trends, and apparently exhibit more than one peak. The difference between yield strength and tensile strength, which is indicative of the ability of the material to work harden, when plotted against temperature (Fig. 4(b)) however clearly shows that there is only one peak, centered at ~823 K. This strongly suggests that in the present material, a single mechanism is responsible for DSA. The temperature dependence of ductility is shown in Fig. 5(a). Uniform elongation was highest at 300 K and decreased with increase in test temperature, with a peak at an intermediate temperature regime of 723–873 K. In contrast, with increase in temperature, total elongation first increased and then decreased, with apparently two peaks, the first one at the same temperature range as for uniform elongation, i.e., 723–873 K, and the second one at a still higher temperature, ~973 K. The peaks at 723–873 K, clearly correspond to the anomalous variations in strength properties in the same temperature range, and attributable to DSA. However, DSA is known to promote non-uniform deformation, and therefore in the DSA regime, dip rather than peak in uniform elongation would have been expected. This suggests that in the present material, the mechanism is more complex, and probably reflects complex interplay of the recovery of the prior cold work dislocation substructure during deformation at the test temperature with the process of DSA.

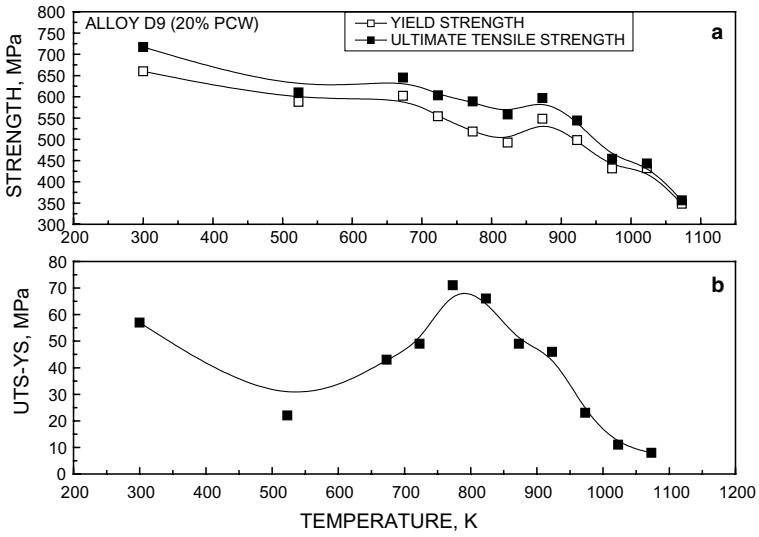

Fig. 4. Variation of (a) yield strength (YS), ultimate tensile strength (UTS) and (b) UTS-YS with temperature for 20% prior cold worked Alloy D9.

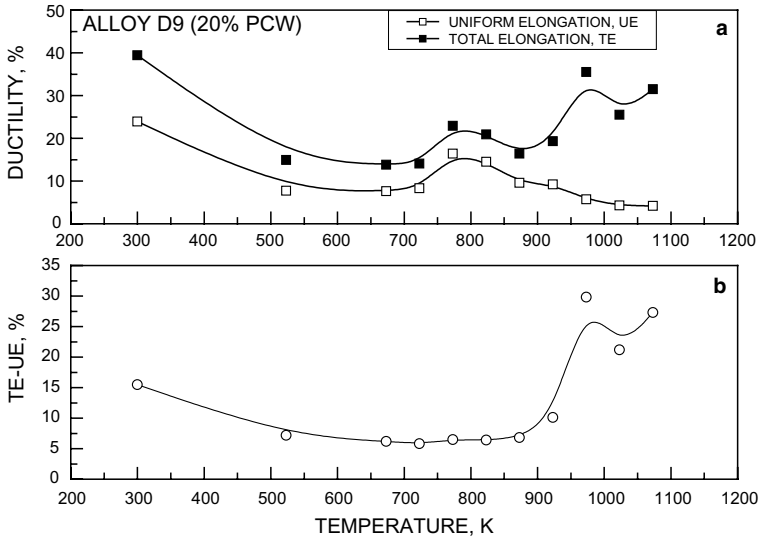

Fig. 5. Variation of (a) uniform elongation (UE), total elongation (TE) and (b) TE–UE with temperature for 20% prior cold worked Alloy D9.

This, plus enhanced recovery of the prior cold worked structure with increasing test temperature might be the reason for the second peak in the total elongation at a higher temperature. With increase of test temperature, the post-necking elongation, i.e., the difference of total and uniform elongations, initially decreased to a minimum at ~773 K, and then increased. Obviously, DSA in the temperature range 773–873 K has only marginal effects on post-necking elongation. A strong peak is however seen at ~973 K. Since post-necking regime is dominated by processes of gross micro-void nucleation, growth and coalescence, which are responsible for ductile fracture, it is worthwhile carrying out more detailed research on the anomalous temperature dependence of ductility parameters, particularly the post necking elongation, in the present material.

Of the several empirical relations proposed in the literature relating tensile flow stress to plastic strain in engineering materials, the Hollomon equation [22], Eq. (2), has been the most popular. In most of the engineering materials this relation is valid only beyond a few percentage strain. Recently Samuel and Rodriguez [31] have shown that this can be attributed to a very small 'equivalent plastic strain', ε_0 characteristic of the structure present in the material and a relation $\sigma = k(\varepsilon + \varepsilon_0)^n$ should describe the entire stress strain curve. The tensile data upto the necking generated in the present campaign were analyzed using Eq. (2). For the serrated flow regime, average stress values were used for this purpose; this recognizes that when Luders strain is absent, the serrations reflect only spatially and temporally local modulations of the overall deformation behavior. Least square fit was used to determine the k and n values in Eq. (2). Fig. 6(a) and (b) show their variations with temperature. Fig. 6(c) shows the temperature dependence of volumetric plastic strain energy density for uniform deformation E_p, computed as

$$E_p = \int_0^{\varepsilon_u} \sigma \, d\varepsilon = k\varepsilon_u^{(n+1)}/(n+1) = kn^{(n+1)}/(n+1) \tag{3}$$

where ε_u is the true plastic strain at the point of maximum load. E_p is the maximum plastic work that can be imparted to the tensile specimen before inhomogeneous deformation in the form of necking intervenes. All three parameters generally decrease with increase in temperature, and show anomalous increase in the form of peaks in the temperature regime for DSA which are particularly strong for n and E_p. At 300 K, the value of n for the cold worked material (0.13) is considerably lower than the range of 0.35–0.37 reported for solution annealed D9 materials with various Ti/C ratios [11], consistent with higher initial dislocation density in the cold worked material. The peaks in the variations of k and n with temperature are similar to the behavior observed in type 316 stainless steels in the DSA temperature range.

Srinivas et al. [32,33] have shown that DSA increases ductile fracture toughness in single phase materials, when micro-voids leading to ductile

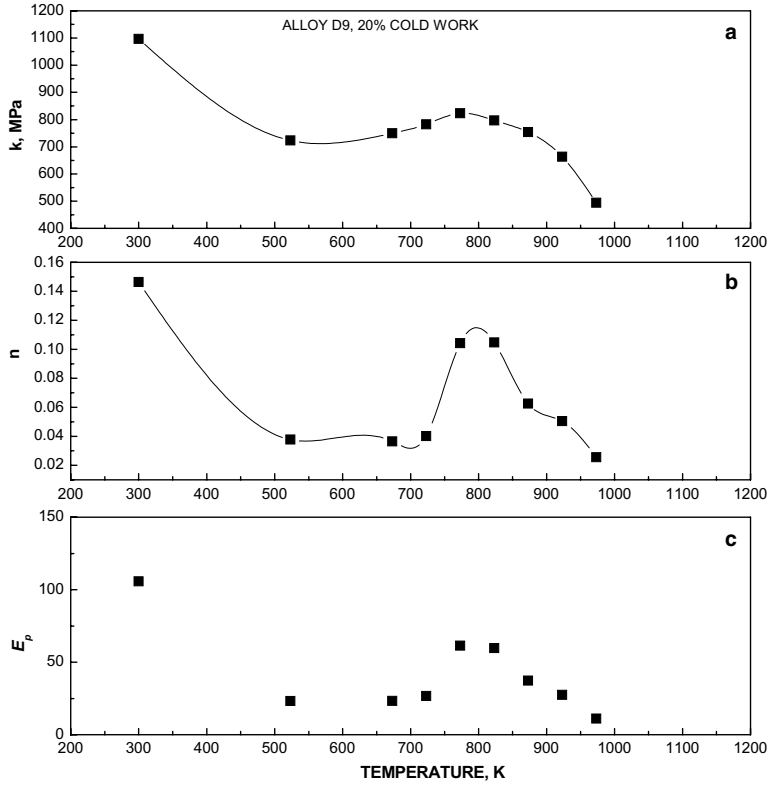

Fig. 6. Variation of (a) strength coefficient k, (b) strain hardening index n and (c) volumetric plastic strain energy density as a function of test temperature for 20% prior cold worked Alloy D9.

fracture nucleate at grain boundaries because of impingement of slip bands. Linga Murty [34] showed that in Armco iron, fracture energy increases in the DSA temperature region. Ray et al. [35] have shown that at ambient temperature, strain ageing in solution annealed stainless steel type AISI 316 (due to pipe-diffusion of C atoms [36]) increases energy absorbed by the material in the post-necking regime of deformation up to fracture. These results are consistent with the above conclusion. However, Choudhary et al. [37] reported that in 9Cr–1Mo steel in normalized and tempered condition, DSA gives rise to a small increase in E_p. The extent of increase in E_p in the present instance is however considerably higher. This can be rationalized noting that while the 9Cr–1Mo steel has a profusion of fine carbide precipitate particles inside the matrix, the D9 Alloy matrix is essentially free from precipitates (except for any precipitation during the high temperature tensile testing which however should not be significant). The sharp increase in E_p, and also the anomalous increase in post necking elongation (Fig. 5(b)) for the present material strongly suggest that in this essentially precipitate free material, DSA would significantly improve ductile fracture toughness of the material. This is a technologically important area, meriting closer scrutiny.

4. Conclusions

The following conclusions could be derived from the present study.

1. Prior cold worked alloy D9 shows serrated plastic flow in a narrow temperature region of 773–873 K compared to that of solution annealed material.
2. The strength and ductility of a prior cold worked alloy D9 show anomalous variation with test temperature in the DSA regime.
3. The strength coefficient k and strain hardening exponent n with temperature show anomalous variation in DSA temperature regime.
4. The plastic strain energy density for homogeneous deformation shows a peak in the dynamic strain ageing temperature showing that DSA in cold worked alloy D9 might be beneficial for ductile fracture resistance.

5. It is suggested that the difference in the ultimate tensile strength and yield strength, plastic strain energy density are handy tools for identifying DSA regime.
6. Though the mechanism of DSA is not identified conclusively, the estimate of the apparent activation energy (97 kJ/mol) and also literature data suggest that pipe diffusion of solute atoms (C, N) through the dislocation core might be responsible for serrated yielding in this temperature range.

References

[1] R.J. Puigh, M.L. Hamilton, in: F.A. Garner, C.H. Henager Jr., N. Igata (Eds.), Influence of Radiation on Material Properties Part II, STP, 956, ASTM, Philadelphia, PA, 1989, p. 22.
[2] D.L. Smith, J. Nucl. Mater. 122 (1984) 51.
[3] W. Kesternich, J. Rothaut, J. Nucl. Mater. 104 (1981) 845.
[4] D.R. Harries, Nucl. Energy 17 (1978) 301.
[5] T. Ikai, S. Yuhara, I. Shibara, H. Kubota, M. Itoh, S. Nomura, in: Proceeding of the International Conference on Materials for Nuclear Reactor Core Applications, BNES, London, 1987, p. 203.
[6] C.F. Jenkins, G.V. Smith, Trans. Metall. Soc. AIME 245 (1969) 2149.
[7] E. Pink, Trans. Metall Soc. AIME 245 (1969) 2597.
[8] K.G. Samuel, S.L. Mannan, P. Rodriguez, Acta Metall. 36 (1998) 2323.
[9] S.L. Mannan, K.G. Samuel, P. Rodriguez, Trans. Ind. Inst. Metals. 36 (1983) 313.
[10] P. Rodriguez, Bull. Mater. Sci. 6 (1984) 653.
[11] S. Venkadesan, PhD thesis, Indian Institute of Technology, Chennai, 1991.
[12] A.H. Cottrell, Dislocations and Plastic Flow in Crystals, Clarendon, Oxford, 1953.
[13] P.G. McCormick, Acta Metall. 20 (1972) 351.
[14] S. Venkadesan, C. Phaniraj, P.V. Sivaprasad, P. Rodriguez, Acta Metall. Mater. 40 (1992) 569.
[15] I.S. Kim, E.O. Hall, Metals Forum 1 (1978) 95.
[16] I.S. Kim, M.C. Chaturvedi, Metals Sci. 13 (1979) 691.
[17] K.W. Qian, R.E. Reed-Hill, Acta Metall. 31 (1983) 87.
[18] M.C. Chaturvedi, D.J. Lloyd, Mater. Sci. Eng. 58 (1983) 107.
[19] C.F. Jenkins, G.V. Smith, J. Iron Steel Inst. 206 (1968) 1267.
[20] Kaiping Peng, Kuangwu Qian, Wenzhe Chen, Mater. Sci. Eng. A379 (2004) 372.
[21] G. Saada, Electron Microscopy and Strength of Crystals, Inter Science, New York, 1963, p. 651.
[22] H. Hollomon, Trans. AIME. 162 (1945) 268.
[23] M.T. Jovanovic, D. Vracaric, D. Markovic, S. Tadic, Scripta Metall. Mater. 24 (1990) 547.
[24] K. Mukerjee, C. D' Antonio, R. Maciag, G. Fischer, J. Appl. Phys. 39 (1968) 5434.
[25] J. Guillot, J. Grilhe, Acta Metall. 20 (1972) 291.
[26] L.P. Kubin, Y. Estrin, Acta Metall. Mater. 38 (1990) 697.
[27] L.J. Cuddy, W.C. Leslie, Acta Metall. 20 (1972) 1157.
[28] C. Gupta, J.K. Chakravarthy, S.L. Wadekar, J.S. Dubey, Mater. Sci. Eng. A 292 (2000) 49.
[29] I.S. Kim, M.C. Chaturvedi, Mater. Sci. Eng. 37 (1979) 165.
[30] K.G. Samuel, S.L. Mannan, P. Rodriguez, J. Mater. Sci. Lett. 15 (1996) 1697.
[31] K.G. Samuel, P. Rodriguez, J. Mater. Sci. 40 (2005) 5727.
[32] M. Srinivas, G. Malakondaiah, R.W. Armstrong, P. Rama Rao, Acta Metall. Mater. 39 (1991) 807.
[33] M. Srinivas, G. Malakondaiah, K. Linga Murty, P. Rama Rao, Scripta Metall. Mater. 25 (1991) 2585.
[34] K. Linga Murty, J. Nucl. Mater. 270 (1999) 115.
[35] S.K. Ray, A.K. Bhaduri, P. Rodriguez, J. Nucl. Mater. 200 (1993) 70.
[36] S.K. Ray, K.G. Samuel, P. Rodriguez, Scripta Metall. 27 (1992) 271.
[37] B.K. Chowdhary, S.K. Ray, K. Bhanu Sankara Rao, S.L. Mannan, Berg und Huttenmannische Monatshefte (BHM) 137 (1992) 439.
[38] R. Tamhankar, J. Plateau, C. Crussard, Rev. Metall. 55 (1958) 383.
[39] J.T. Barnby, J. Iron Steel Inst. 204 (1966) 23.
[40] K.S.B. Rose, S.G. Glover, Acta Metall. 14 (1966) 1505.
[41] L.H. De Almeida, I. Le May, S.N. Monteiro, in: H.J. McQueen, J.P. Bailon, J.I. Dickson, J.J. Jones, M.G. Akben (Eds.), Strength of Metals and Alloys (ICSMA 7), vol. 1, Pergamon, Oxford, 1986, p. 337.
[42] D. Blanc, J.L. Strudel, in: H.J. McQueen, J.P. Bailon, J.I. Dickson, J.J. Jones, M.G. Akben (Eds.), Strength of Metals and Alloys (ICSMA 7), vol. 1, Pergamon, Oxford, 1986, p. 349.
[43] R. Ilola, M. Kemppainen, H. Hanninen, Mater. Sci. Forum 318–320 (1999) 407.
[44] A. Gironès, L. Llanes, M. Anglada, A. Mateo, Mater. Sci. Eng. A 367 (2004) 322.
[45] Seong-Gu Hong, Soon-Bok Lee, J. Nucl. Mater. 340 (2005) 307.